

## A Study of Thermal Effects in RF-MEM-Switches using a Time Domain Approach

Werner Thiel, Kelly Tornquist, Ron Reano and Linda P.B. Katehi  
University of Michigan, Ann Arbor, Michigan, 48109, USA

**Abstract** A thermal analysis of RF-MEM-Switches based on the heat conduction is presented. The heat equation is solved by employing a Forward Time Centered Space (FTCS) difference scheme. For the electromagnetic (EM) characterization, the standard FDTD method is used which provides the dissipated RF power in the MEMS metal structure for a subsequent separate heat analysis. The computed temperature distribution in the switch was utilized as an input to a mechanical simulator for a mechanical analysis. This analysis has shown that when the MEMS switch operates under high power, a temperature gradient develops on the structure that strongly affects stress distribution on the switch. This stress redistribution impacts operation and affects switch lifetime. The accuracy of the presented method is demonstrated by comparing the theoretically computed and experimentally verified thermal profile of a patch antenna.

### I. INTRODUCTION

For the past few years, micromechanical systems (MEMS) have become more and more important and have successfully been integrated in RF-circuits up to 40 GHz. Most of these switches have operated under low power conditions in order to improve reliability and extend lifetime. Recent work has demonstrated that for particular capacitive switch architectures, operation under high power is not compromised by self activation but by other effects primarily attributed to redistribution of the mechanical stresses. This redistribution, results in a constant increase of the required activation voltage during switch operation, accelerates dielectric charging and results in a catastrophic failure. When operating under high RF power, the finite electrical conductivity of the metallic structure of the switch creates hot spots which vary with the on or off position of the switch. To be able to understand the phenomena underpinning the observed behavior, the heat transfer in the membrane has to be studied extensively and to be taken into account for a proper design.

As shown by literature, most MEMS are fairly small and physically complicated three dimensional structures. As a consequence, a fully 3D simulation of the heat problem is required to determine the temperature distribution and locate critical points on the MEMS metallic membrane. The temperature influences the stress resulting in a considerable bending of the membrane and affects the actuation voltage, the hysteresis and consequently the time constant of the mechanical

system. These thermal effects are primarily responsible for device failure under high RF power.

For MEMS switches operating in the GHz region where the mechanical, thermal and electromagnetic time constants strongly differ, the system is almost decoupled and can be analyzed iteratively. In the first section, a formulation for the conductive heat equation is given. The dissipated RF-power required as an input for the heat problem is achieved by the standard FDTD analysis described in section III. After the calculation of the temperature variations on the switch, a mechanical analysis is performed to investigate the warping of the switch based on the calculated temperature profile. For validation, a temperature distribution of a patch antenna in the X-band is compared to the simulation results.

### II. THEORETICAL FORMULATION

In this section, conduction is considered as the major mechanism of heat transfer in the thermal analysis of the MEM-switch. Radiation only plays an important role for high temperatures and materials with low conductivity and can therefore be neglected in this application. Another mechanism of heat transfer is the convection, which can easily be employed to the boundaries of the computational domain. Modeling of convection within a structure requires a solution of the airflow in the entire domain resulting in a very complex mechanical system. The general heat conduction equation [1, 2] for the proposed heat analysis is given by

$$c_p \rho \frac{\partial T}{\partial t} = \nabla \cdot (\sigma \nabla T) + H \quad (1)$$

where  $\rho$  is the density,  $c_p$  is the specific heat,  $T$  the temperature,  $\sigma$  the thermal conductivity and  $H$  the dissipated electric power. To solve this parabolic partial differential equation, the Forward-Time Centered-Space (FTCS) scheme [3] is applied.

As the heat simulation is performed after the FDTD simulation, the same grid is chosen for the heat conduction equation. Fig. 1 shows the temperature nodes embedded in the Yee scheme [4]. The temperature nodes are placed in the center of the Yee-cell which defines the control volume for the flux in each spacial direction.

In addition, suitable boundary conditions are required to terminate the domain. The considered boundary conditions strongly affect the rise in temperature and the resulting ther-

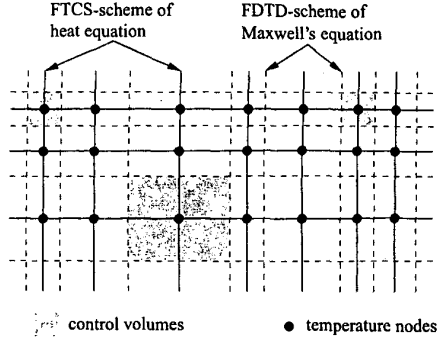


Figure 1: Grid for thermal simulation derived from the Yee-scheme

mal profile because all the heat generated in the structure has to be conducted through the boundaries of the domain. Here, two different kinds of mechanisms are considered. Based on the fact that the circuit is attached to a wafer with high conductivity mounted on a heat sink, a constant temperature boundary condition can be applied on the bottom surface. The surface on the top is more difficult to handle because the air-flow and its temperature has to be modeled correctly. In the simplest case, such a convective boundary condition can be formulated by the following equation:

$$\frac{\partial T}{\partial n} = \frac{h}{\sigma} (T_B - T_A) \quad (2)$$

where  $n$  is the normal vector,  $h$  is surface heat transfer coefficient and  $T_B$  and  $T_A$  is the temperature of the boundary node and the fluid, respectively.

### III. EM-ANALYSIS OF MEMS

In this section, the source term  $H$  of equation (1) is specified by performing a FDTD analysis [4]. The dissipated RF-power in the MEMS membrane is the dominating factor for the heat generation process whereas the ohmic losses in the transmission line and in the substrate have a minor influence. The source term in the heat equation is given by  $H = \vec{j} \cdot \vec{E}$ . In general, the thickness of the membrane is larger than the skin depth at the frequency of interest. As a consequence, an effective conductivity [5, 6]

$$\sigma_{eff} = \sigma \frac{2}{d\sqrt{j\omega\mu\sigma}} \tanh\left(\sqrt{j\omega\mu\sigma} \frac{d}{2}\right) \quad (3)$$

has to be introduced to the membrane. As an alternative, a resistive sheet [6] with the corresponding surface impedance can also be applied. In this approach, the inductive part of the skin-effect is not taken into account. Fig. 2 shows a photograph of the analyzed MEMS switch. The losses in the

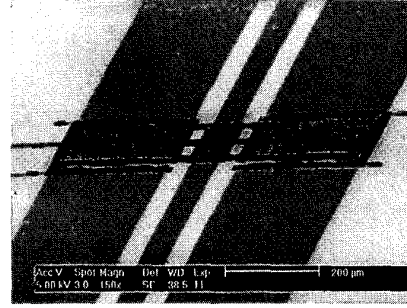


Figure 2: Fabricated and analyzed MEMS switch.

MEMS structure are determined in two different ways. First, the total loss is extracted from the scattering parameters pictured in Fig. 3. The diagram shows the losses when the membrane is in the up and down position. Then, the ohmic

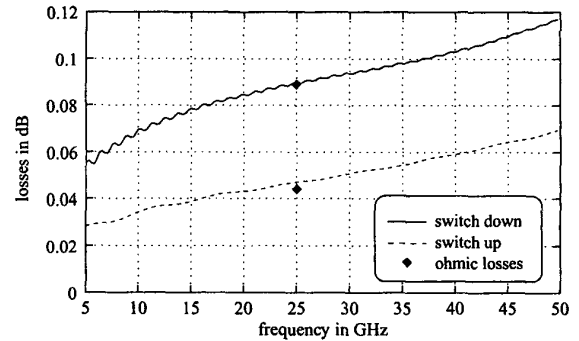


Figure 3: Dissipated power in the Ni-membrane versus losses extracted from the scattering parameters.

losses in the MEMS membrane are calculated at 25 GHz. These losses appear as points in Fig. 3. In conclusion, the total loss of the MEMS switch is caused by the ohmic loss in the membrane and radiation effects are negligibly small. The current distribution on the membrane for both operating states is shown in Fig. 4 and Fig. 5. When the membrane is down, the current only concentrates on the front edge of the first bridge due to the skin-effect. Because the MEMS switch presents an RF short for the incoming wave, the electric field in the slot of the CPW line decays fast and does not cause further significant currents in the other bridges. A different current pattern can be observed when the membrane is up. In the up position, two hot spots on the first and the last bridge are obtained because the RF-power is transmitted and therefore, the electric field is constant underneath the entire length of the membrane along the CPW slot. According to Fig. 3, the ohmic losses in the MEMS membrane are only increased

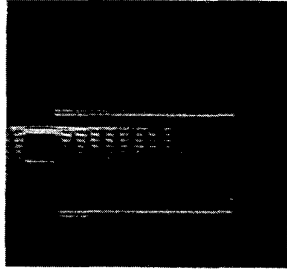


Figure 4: Current distribution in the Ni-membrane in the down position

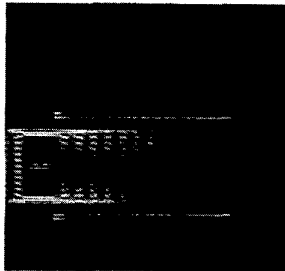


Figure 5: Current distribution in the Ni-membrane in the up position

by a factor two when the membrane is up.

#### IV. HEAT ANALYSIS OF MEMS

A heat analysis of the MEMS switch (Fig. 2) has been carried out for an RF-input power of 1 W. According to Fig. 3, the ohmic losses in the membrane result in 10.1 mW and 20.3 mW for the up and down states of the switch, respectively. A steady state is achieved after about 1 ms for the down state, and a slightly longer transient is observed in the up state. The heat analysis leads to two different temperature distributions which are illustrated in Fig. 6 and Fig. 7.

When the switch is in the down position, only a hot spot appears in the bridge where also the current has its maximum. Hence, the heat is directly conducted through the thin dielectric layer into the Si-substrate due to the thermal contact between the two materials. Furthermore, the Si-substrate acts as a heat sink and conduction is the major part of the heat transfer. A different pattern is achieved, when the switch is released. Now the membrane is practically surrounded by air and almost isolated due to its small thermal conductivity. Hence, the membrane heats up and hot spots are spread out. In practice, an airflow through the membrane will be the main component of the cooling mechanism. Thus, the temperature distribution for the up state shown in Fig. 7 is the worst case

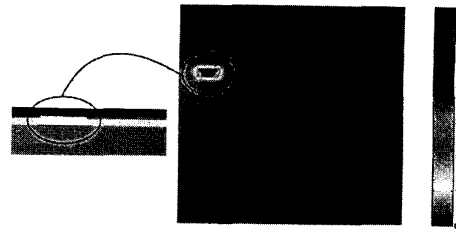


Figure 6: Temperature distribution in the Ni-membrane in the down position; diagram shows rise of temperature in Kelvin.

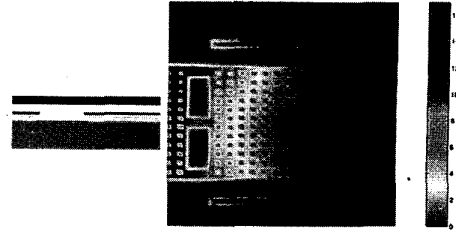


Figure 7: Temperature distribution in the Ni-membrane in the up position; diagram shows rise of temperature in Kelvin.

for the heating process.

#### V. MECHANICAL ANALYSIS

Because thermal, mechanical, and electromagnetic time constants are different by orders of magnitude, the various responses of the switch are weakly coupled. This allows an iterative approach in the solution of the individual problems, so that the hotspots from the thermal analysis were utilized as thermal sources in a mechanical model [7] to determine the affects of high temperature gradients on the switch membrane.

In the case of a switch operating under 6.6 W of RF power, a maximum temperature of 411.8 K (118.8 above room temperature) at the location of the hotspot has been calculated. The operating RF power of 6.6 W, has been found experimentally not to cause melting or self-actuation [9]. This temperature of 411.8 K was then placed as a thermal source on the air bridges to simulate the heat distribution obtained in the thermal analysis. With steady state conditions assumed, the mechanical equations [7] determined that this particular high temperature caused substantial warping of the switch membrane (Fig. 2). The scale of displacement is in micrometers, but the displacement shown pictorially has been exaggerated to account for an aspect ratio of the switch membrane of 320:1. As it is evident from the picture, the RF power causes stress redistribution which causes a substantial deflection of the center of

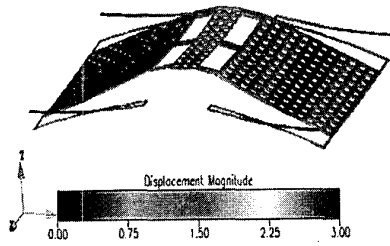


Figure 8: Switch warping not shown to scale.

the switch and results in a substantial increase of the gap. This separation as measured between the center of the bottom and top dc electrodes used to electrostatically activate the switch is approximately 3.75 microns. The gap between the center of the switch and the center of the CPW line is as high as 5 microns. The initial gap size of 3 micrometers has a theoretical pull down voltage of 3.9 V. However, the increase in gap size, from 3 to 3.75 micrometers, can drastically increase the pull down voltage to 5.45 volts representing an increase of 39.7% as given by

$$V_{pi} = \frac{\sqrt{8K_z g_0^3}}{27A\epsilon_0} \quad (4)$$

where  $A$  is the area of the electrodes,  $g_0$  is the gap size, and  $K_z$  is the spring constants of the meanders. This calculation does not include the increase in the spring constants of the meanders caused by the warping of the meanders themselves, which would also contribute to an additional increase in the actuation voltage. This thermal analysis explains the higher voltages measured [9].

## VI. VALIDATION

In order to validate the above mentioned simulation technique, the thermal profile of an X-band patch antenna was measured experimentally using a EO/thermal probe whose design was based on semiconductor bandgap thermometry. The optical transmissivity through the probe is modulated by variations in probe temperature due to the temperature dependence of the bandgap. Using standard micromachining technology, small dimension probes are obtainable, allowing the possibility to produce thermal images with a spatial resolution on the order of tens of microns.

Complete details of the experimental technique can be found in [10]. The acquired thermal image was found to be in good agreement with the results obtained from simulations. A large hot spot is observed in the vicinity of the microstrip feed where the temperature peaks at 40 degree Centigrade. The temperature distribution is seen to fall away rapidly with lateral distance from the antenna, indicating a good flow of heat

from the antenna to its heat sink. A sensitivity analysis of the loss mechanisms show that dielectric loss dominates the temperature distribution above the patch. Similar thermal images will be acquired above MEMS switches in order to validate the simulation results.

## CONCLUSION

A thermal analysis of a RF-MEM-Switch based on a FDTD approach was presented in this paper. The dissipated power was achieved by a previous FDTD simulation and the thermal problem was solved by applying a FTCS scheme to the heat conduction equation. The temperature distribution was used as an input for a further mechanical modeling to investigate the impact of the heating on the actuation voltage. The thermal analysis was validated by a measured temperature profile of an antenna patch in the X-band and compared to the simulation results.

## ACKNOWLEDGEMENT

This work has been funded by the MARRS/MURI program "Multifunctional Adaptive Radio, Radar and Sensors" (2001-0694-02).

## REFERENCES

- [1] A.J. Chapman, *Fundamentals of Heating Transfer*, New York: McMillan Publishing Comp., 1987.
- [2] E. Cardelli, M. Gimignani and M. Raugi, "Numerical modelling of 3-D Coupled Electromagnetic and Heating Diffusion Problems", *IEEE Trans. Magnetics*, vol. 30, no. 5, pp. 3335-3338, September 1994
- [3] J.W. Thomas, *Numerical Partial Differential Equations, Finite Difference Methods*, New York: Springer, 1995.
- [4] K.S. Yee, "Numerical Solution of Initial Boundary Value Problems Involving Maxwell's Equation in Isotropic Media", *IEEE Trans. Antennas Propagation*, vol. 14, no. 5, pp. 302-307, May 1966.
- [5] W. Thiel, "A Surface Impedance Approach for Modeling Transmission Line Losses in FDTD", *IEEE Microwave guided Wave Lett.*, vol. 10, no. 3, pp. 89-91, March 2000.
- [6] A. Lauer and I. Wolff, "A conducting sheet model for efficient wide band FDTD analysis of planar waveguides and circuits", *Microwave Symp. Dig.*, 1999, pp. 1589-1592.
- [7] Coventorware software version 2001.3 with the MemMech solver using the ThermalMech Tool.
- [8] S.P. Pacheco, D. Peroulis and L.P.B. Katehi, "MEMS single-pole double-throw (SPDT) X and K-band switching circuits", *Microwave Symp. Dig.*, 2001, pp.941-944.
- [9] S.P. Pacheco, L.P.B. Katehi and C.T.-C. Nguyen "Design of low actuation voltage RF MEMS switch", *Microwave Symp. Dig.*, 2000, pp. 165 -168.
- [10] R. Reano, K. Yang, J. F. Whitaker, L. P. B. Katehi "Integrated electro-thermal probe", *2001 IEEE MTT-S Int. Microwave Symp. Dig.*, vol. 3, pp. 1523-1526, May 2001.